Mater. Res. Soc. Symp. Proc. Vol. 1107 © 2008 Materials Research Society

Modelling Transport of ^{14}C-Labelled Natural Organic Matter (NOM) in Boom Clay

Alice Ionescu[1], Norbert Maes[2], and Dirk Mallants[2]
[1]Agency for Radwaste Management (ANDRAD), Str. Campului 1, Mioveni 115400, Romania
[2]Belgian Nuclear Research Centre (SCK•CEN), Boeretang 200, 2400 Mol, Belgium

ABSTRACT

In Belgium, the Boom Clay formation is considered to be the reference formation for HLW disposal R&D. Assessments to date have shown that the host clay layer is a very efficient barrier for the containment of the disposed radionuclides. Due to absence of significant water movement), diffusion - the dominant transport mechanism, combined with generally high retardation of radionuclides, leads to extremely slow radionuclide migration. However, trivalent lanthanides and actinides form easily complexes with the fulvic and humic acids which occur in Boom Clay and in its interstitial water. Colloidal transport may possibly result in enhanced radionuclide mobility, therefore the mechanisms of colloidal transport must be better understood. Numerical modeling of colloidal facilitated radionuclide transport is regarded an important means for evaluating its importance for long-term safety.

The paper presents results from modeling experimental data obtained in the framework of the EC TRANCOM-II project, and addresses the migration behavior of relevant radionuclides in a reducing clay environment, with special emphasis on the role of the Natural Organic Matter (NOM) [1]. Percolation type experiments, using stable ^{14}C-labelled NOM, have been interpreted by means of the numerical code HYDRUS-1D [2]. Tracer solution collected at regular intervals was used for inverse modeling with the HYDRUS-1D numerical code to identify the most likely migration processes and the associated parameters. Typical colloid transport submodels tested included kinetically controlled attachment/detachment and kinetically controlled straining and liberation.

INTRODUCTION

Normally, in reducing clay environments, low values of mobile radionuclide concentrations in the clay pore-water are due mainly to solubility limitation. However, the presence of NOM may enhance the solubility due to complexation/colloid formation and/or may influence the sorption behaviour of radionuclides. Transport processes characteristics of Boom Clay were investigated by means of laboratory and in-situ experiments, taking account of NOM. In this paper, a set of laboratory migration experiments was carried out to clarify the possible role of mobile NOM as radionuclide carrier. For this purpose, radionuclide sources (^{241}Am) were prepared with concentrations as close as possible to their expected equilibrium concentration under in-situ Boom Clay conditions and in contact with ^{14}C-labeled BC Organic Matter (^{14}COM), so-called "double-labeled" migration experiments (details can be found in [1,3]). This paper focuses on the migration of the ^{14}COM. Breakthrough data of the ^{14}C labeled OM from these percolation experiments were used to inversely estimate meaningful values for migration parameters capable of describing colloid transport (sorption, attachment/detachment rates, straining).

MATERIALS AND METHODS

In so-called percolation type migration experiments, the radionuclide source is brought on a filter paper and confined between two clay cores. At one end, real Boom Clay water (RBCW) is forced into the clay core under constant pressure while at the other end percolating fluid is collected for monitoring. Characteristics of the experimental set-up are given in Table I. Further note that the percolation experiments were done with a fixed total plug length but with varying end-plug lengths (i.e., distance of the source to the outlet of the clay core), and varying Darcy velocities (Table II). The ^{14}C-labeled OM solution is characterized by large molecular weight molecules (30 000 MWCO), and the OM particle sizes range between 2.1 and 5 nm [1].

Table I. Experimental details for percolation tests.

Parameter	Data
Length of the clay core (cm)	7.2
Cross-sectional area, S (cm^2)	11.34
Length of the filter (cm)	0.2
Filter porosity, η (-)	0.4
Filter bulk density, ρ_b (g cm^{-3})	1.7
Used amount of source solution (cm^3)	0.2
Recovered activity at the outlet (%)	See Table II
Average flow rate, Q (cm day^{-1})	
Pore-water diffusion coefficient D_p (cm^2 day^{-1})	0.0432
Tracer half life, $T_{1/2}$ (days)	2.094×10^6
Source activity concentration, corrected for losses (Bq cm^{-3}), $C_0 = A_0/VOL$	18.1
Saturated water flux (Darcy velocity), $q_D = Q/S$ (cm day^{-1})	See Table II

Table II: Overview of Am-OM double labeled data. Travel length is distance between source (M2) and outlet (more details in [1, 3]).

Experiment code	Travel length, TL (cm)	Experiment duration, T (d)	Average flow rate, Q (cm^3/d)	Hydraulic conductivity, K_h (10^{-12} m/s) [P (MPa)]	Recovered ^{14}C activity (Bq)
ShortPAmCOM	1.2	620	0.164	1.3 [0.94]	2 720 (60.1 %)
LongPAmCOM	6.0	620	0.185	1.5[0.91]	2147 (59.2 %)
HiPAmCOM	3.6	620	0.173	0.9 [1.29]	2170 (59.8 %)
MePAmCOM	3.6	621	0.393	2.9[0.94]	2610 (72 %)
LowPAmCOM	3.6	621	0.304	2.5[0.85]	2650 (73.1 %)

THEORY AND MODELS

Colloid transport may be described by a combination of the convection-dispersion-retardation equation and colloid attachment theory [2]:

$$\frac{\partial(\eta_e c)}{\partial t} + \rho\frac{\partial(s_e)}{\partial t} + \rho\frac{\partial(s_1)}{\partial t} + \rho\frac{\partial(s_2)}{\partial t} = \frac{\partial}{\partial x}\left(\eta_e D\frac{\partial c}{\partial x}\right) - \frac{\partial(q_D c)}{\partial x} - \mu_w\eta c - \mu_s\rho(s_e + s_1 + s_2) \qquad (1)$$

where c is the colloid concentration in the aqueous phase [N_c cm^{-3}], ρ is the bulk density (g cm^{-3}), s is the colloid solid phase concentration [N_c g^{-1}], subscripts e, 1 and 2 represent equilibrium and two kinetic sorption sites, respectively, N_c is the number of colloids, μ_w and μ_s represent decay rates in the liquid and solid phases (d^{-1}), respectively, t is time (d), $D = D_P+\alpha\times v$ is hydrodynamic dispersion coefficient (cm^2 d^{-1}), D_p is diffusion coefficient (cm^2 d^{-1}), α is dispersivity (cm), q_D is Darcy flux (cm d^{-1}), η_e is effective porosity (-), $v=q_D/\eta_e$ is pore-water velocity *(*cm d^{-1}*)* λ is the decay constant (d^{-1}), and x is distance (cm).

Considering the flexibility in the modeling by using a non-linear sorption model, the Freundlich sorption isotherm relating dissolved (c) and adsorbed (s) concentrations has been used in the present model:

$$s = k_F \cdot c^b \qquad (2)$$

where b is the Freundlich exponent (-) and k_F is the Freundlich sorption coefficient (cm^3 g^{-1}).

Mass transfer between the aqueous and solid kinetic phases can be described as (the indexes 1, respectively 2, have been dropped in the following equation)

$$\rho \frac{\partial s}{\partial t} = \eta_e k_a \Psi c - k_d \rho s \qquad (3)$$

accumulation on solid phase *attachment / straining* *det achment / liberation*

where k_a is the first-order deposition (attachment) coefficient [d^{-1}], k_d is the first-order entrainment (detachment) coefficient [d^{-1}], and Ψ is the colloid retention function [-] (see further). Attachment is the removal of colloids from solution via collision with and fixation to the solid phase, and it is dependent on colloid-colloid, colloid-solvent, and colloid-porous media interactions [4, 5]. To simulate reductions in the attachment coefficient k_a as a result of filling of favorable attachment sites, a Langmuirian dynamics equation may be used to describe the decrease of Ψ with increasing colloid mass retention (~blocking mechanism) [2]

$$\psi = 1 - S / S_{max} \qquad (4)$$

where S_{max} is the maximum solid phase concentration [N_c g^{-1}]). Alternatively, a depth-depending blocking coefficient may be invoked to characterize the so-called straining process, where straining means the entrapment of colloids in down gradient pores and at grain junctions that are too small to allow particle passage [2]:

$$\psi = \left(\frac{d_c + x - x_0}{d_c} \right)^{-\beta} \qquad (5)$$

where d_c is colloid diameter (cm), β is a fitting parameter (-) that controls the shape of the colloid spatial distribution, x is depth (cm) and x_0 is depth of the column inlet or textural interface (cm).

RESULTS AND DISCUSSIONS

Breakthrough curves and application of the attachment-detachment model to experimental data

Observed breakthrough curves for the ^{14}C-labeled OM reveal that peak concentrations and time of the peak (Figure 1) are influenced by 1) the position of the source within the clay core, and 2) by the flow rate, which is highest for MePAmCOM (highest K_h×pressure value) and lowest for HiPAmCOM (lowest K_h×pressure value). (Table II). For similar water fluxes (0.015 – 0.017 cm/d) ^{14}C recovery is independent of travel length and on average about 60%. For the higher flow rates (0.028 – 0.036 cm/d) recovery is higher too (~72-73 %).

For modeling purposes, three sections (materials) have been considered (see Table II for further details): the inlet domain M1, a very thin source layer M2 (0.6 mm long) and the outlet domain M3. The source layer M2 is modeled as a medium with a higher effective porosity (η_e=0.3), in such a way as to accommodate the 200 mm^3 of applied tracer solution containing dissolved ^{14}C-labelled OM.

Size and/or charge exclusion have been taken into account by using an effective porosity, η_e, of 0.13 [1, annex 16], instead of the effective porosity of 0.37 obtained for the conservative tracer HTO [6]. For the dispersivity α, a value of 0.1 mm has been used, based on initial sensitivity analysis (results not shown) [6]. Due to the small duration of the experiments compared to the ^{14}C half life, decay is neglected in the simulation.

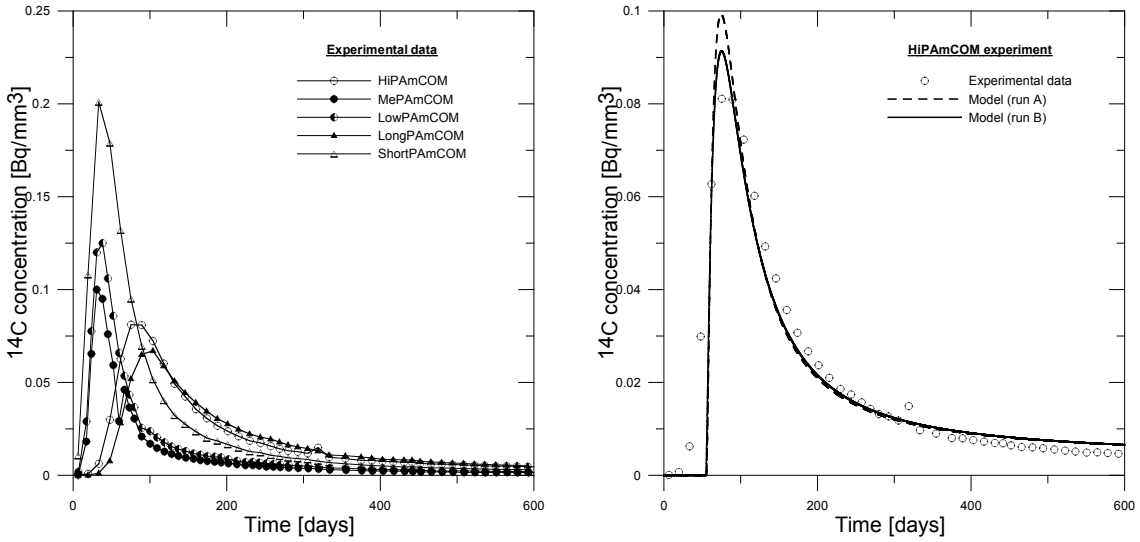

Figure 1: Experimental **^{14}**C labelled OM breakthrough curves (left); fitted and observed **^{14}**C breakthrough curve for HiPAmCOM (right).

The delay of the peak arrival time T_{max}, compared to the advective water travel time through the clay core T_w, in the experimental BTCs suggests the occurrence of a sorption type mechanism for OM transport. The calculated retardation coefficient R varies between 2.4 and 3.1, which suggests mildly retarded OM transport. Based on these retardation values R, Freundlich k_F values were calculated assuming linear reversible sorption. The calculated k_F values were taken as starting values for the inverse calculation with the model based on Eq. 1.

Colloid parameter starting values have been taken from previous calculations, based on simulations with the POPCORN code [1, annex 17], except for the values for the straining and liberation rates, processes that are not modeled within the POPCORN code. Initial sensitivity analysis without considering the detachment (k_{det} = 0, for the attachment-detachment model) and liberation terms (k_{lib} = 0, for the straining model) failed in predicting the observed breakthrough curve (results not shown). Therefore, further calculations always included mechanisms of detachment and liberation.

Modeling ^{14}COM migration

Transport of ^{14}COM is described with an advection–dispersion transport model that accounted for sorption, first-order kinetic attachment–detachment and straining-liberation.

Boundary conditions for ^{14}COM migration consider a zero concentration flux at the inlet and a zero-gradient condition at the outlet. Initial condition is given by the concentration in the source layer M2.

Modeling of the migration of OM was done by considering three different sorption sites: site (1) equilibrium with non-linear Freundlich sorption (submodel 1), site (2) kinetically controlled attachment/detachment (submodel 2) and site (3) kinetically controlled straining and liberation (submodel 3). Part of the ^{14}COM colloids are presumed to be sorbed on the solid surface (the equilibrium site – submodel 1). Sorption is considered to take place both at the inlet and the outlet layers of the clay column, but it is neglected in the thin source layer M2. Colloid attachment (submodel 2) was taken into account in all the three layers (i.e., M1, M2, and M3).

Presence of the Ψ-parameter in the attachment/straining component of the mass-transfer equation (3) allows one to account for different straining/blocking mechanisms. The simulation of the BTC curves for ^{14}COM colloids taking into account advection, dispersion and 'clean-bed' attachment-detachment model ($\Psi = 1$ and $k_d = 0$) for both kinetic sites failed in reproducing both the peak (including peak arrival time) and the tailings of the BTC curves. Introducing nonlinear sorption (Freundlich isotherm with $b = 1.1$) for layer M3 (outlet), resulted in an improvement in matching the peak concentration (including the peak arrival time), but the slow residual release at the tailings was still not met. Therefore, for the first kinetic site, colloid mass removal from solution is considered to take place by Langmuir blocking (Eq. 4). The second kinetic site considers straining (see further). Although the starting values of the attachment/detachment coefficients are the same for both kinetic sites, this may not be necessarily true since attachment depends, among other factors, on colloid-solid and colloid-colloid interactions. Due to the heterogeneity of the solid phase and of the ^{14}COM colloids, the use of different values for the attachment and detachment coefficients may be required. When depth-dependent straining was invoked (submodel 3, Eq. 5) in addition to attachment and detachment, the liberation rate was first set to zero. Taking the straining process into account in the column inlet part is justified by the fact that back-diffusion can divert the ^{14}C-labelled OM from the source zone M2 into the inlet component of the clay column.

Simulations started with the experiment HiPAmCOM. Inverse calculations resulted in a set of parameter values descriptive of colloid transport of OM. The optimized parameters for the HiPAmCOM experiment are then used to simulate the other four experiments (forward calculations).

Inverse calculations for HiPAmCOM experiment (^{14}COM)

Inverse calculations for determination of the advection dispersion transport and colloid model parameters have been performed with the HYDRUS-1D code for the HiPAmCOM experiment. The fitting had to deal with a very large number of parameters for three materials. In a first instance, following parameters were fitted in a staged manner: equilibrium sorption parameters k_F (Freundlich distribution coefficient) and b (Freundlich exponent), effective porosity η_e and dispersivity α in the inlet and outlet layers, site-1 attachment (k_{att1}) and detachment (k_{det1}) rates for the inlet (M1) and outlet (M3) layers of the clay core, attachment ($k_{att1} = k_{att2}$) and detachment ($k_{det1} = k_{det2}$) rates for the source layer M2 (site-1 identical to site-2), site-2 straining (k_{str}) and liberation (k_{lib}) rates for the inlet (M1) and outlet (M3) layers, the medium grain diameter of the clay d_c and empirical factor β in the depth-dependent straining function (Eq. 5). The values that had thus been obtained were kept constant while continuing the fitting

with the next set of two to three parameters, until all parameters were optimized. Final results are referred-to as run A (r^2=0.926). At this stage, no parameter constraints have been imposed during optimization. A second global optimization (run B) has been undertaken where all parameters simultaneously were allowed to vary in a 10% interval from the optimal values obtained in run A. The fitted parameter values for run A and B are shown in Table III, while observed and fitted BTC are displayed in Figure 1. Including the diffusion coefficient D_p in the optimization run B reduces the calculated peak by about 10% and brings it in much better agreement with the data (r^2=0.947), while the tailing of the simulated BTC is now in good agreement with the observed BTC.

Table III: Optimized parameter values in the first (diffusion fixed) and second fit (diffusion optimized). Here NF means 'parameter not fitted', and f stands for 'fixed parameter value'. (units in mm, g and d).

Param.	Layer M1 & M3		Layer M2		Param.	Layer M1 & M3		Layer M2	
	Run A	Run B	Run A	Run B		Run A	Run B	Run A	Run B
η_e	0.14	NF	0.3 (f)	0.3 (f)	k_{det1}	0.0014	0.0012	0.0017	(0.0015)
D_p	4.32 (f)	6.43	4.32 (f)	3.94	k_{att2} (k_{str})	0.1011	0.090	0.017	(0.015)
k_F	83.86	92.01	0 (f)	0 (f)	k_{det2} (k_{lib})	0.010	0.0095	0.0017	(0.0015)
b	0.39	0.43	1 (f)	1 (f)	S_{max2} (β)	0.418	0.45	10^{25} (f)	10^{25} (f)
k_{att1}	0.017	0.015	0.017	(0.016)	d_c	0.0010	0.00095	0.0010	0.00091

Direct calculations for MePAmCOM, LowPAmCOM, ShortPAmCOM and LongPAmCOM experiments (^{14}COM)

The optimized parameters resulting from run A and B were then used to simulate in a direct way the remaining BTCs. It can be seen (from Figure 2 and Table IV) that the forward simulations are in good agreement with the experimental data when the source is located in the middle of the clay column (MePAmCOM, LowPAmCOM), but for experiments with a different position of the source (i.e., LongPAmCOM and ShortPAmCOM), the simulations fail in representing the data for both run 1 (using run A parameters) and run 2 (using run B parameters). Run 2 gave a better agreement with the experimental data for all the simulated experiments, except for the LongAmCOM data for which the model underestimates the peak concentration by more than a factor of 2. The difference is in agreement with the hypothesis of the different structure of the source layer compared to the rest of the column (by assigning a higher porosity). Also, the heterogeneity of the clay and of the organic matter may be accounted for by using different values for the attachment and detachment coefficients for the two kinetic sites in the source layer. For both parameter sets considered, there is a discrepancy between the magnitude and arrival of the first measured and simulated concentration breakthrough (Table IV). For experiment ShortPAmCOM, travel length is 12 mm compared to 36 for HighPAmCOM, while for experiment LongPAmCOM a longer travel length (60 mm) is used. Owing to the resulting difference in travel time, several processes (for example, dispersion, kinetically controlled attachment/detachment, etc) that are distance and/or time dependent may not be well described on the basis of parameter values derived from tests with different space and time scales.

Experiment type	Run no.	Peak ^{14}C concentration [Bq mm^{-3}]		Time of peak [days]		Recovered activity [Bq]		Coefficient of regression
		EXP	CALC	EXP	CALC	EXP	CALC	
HiPAmCOM	1.	0.081	0.098	75.4	74.9	2170	2149	0.926
	2.		0.089		78.2		2207	0.947
MePAmCOM	1.	0.1	0.22	30.7	29.2	2610	2982	0.768
	2.		0.19		32.0		3035	0.825
LowPAmCOM	1.	0.125	0.18	38.3	39.6	2650	2753	0.605
	2.		0.15		43.1		2810	0.485
LongPAmCOM	1.	0.067	0.04	103.7	180.4	2146	1480	0.0006
	2.		0.03		195.7		1360	0.014
ShortPAmCOM	1.	0.20	0.53	33.3	14.4	2720	4923	0.460
	2.		0.45		14.1		5121	0.587

Table IV: Optimization results for HiPAmCOM and the effect of using the fitted parameters for simulating other experiments. Experimental (EXP) and calculated (CALC) results.

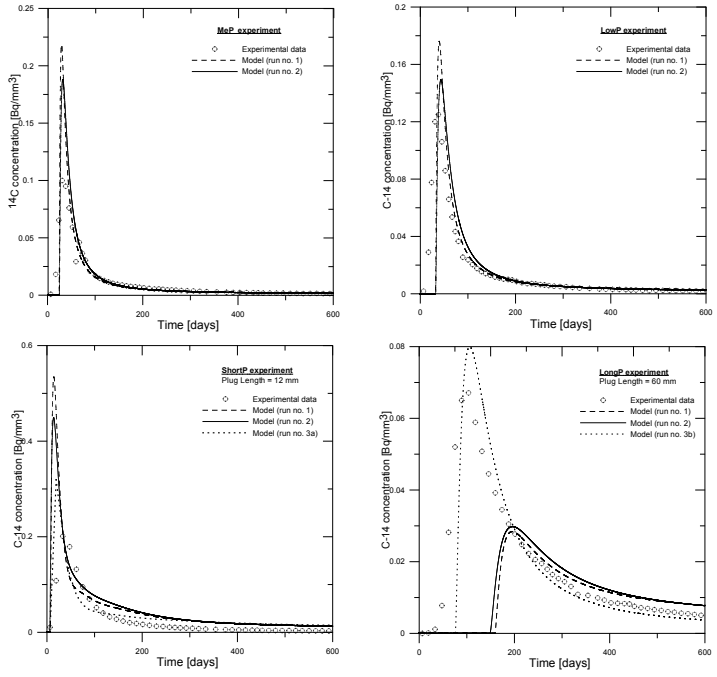

Figure 2: Simulated BTC for MePAmCOM, LowPAmCOM, ShortPAmCOM, and LongPAmCOM experiments, using fitted parameters from HiPAmCOM experiment.

Additional sensitivity analyses have shown that the most influential parameters for the ShortP- and LongPAmCOM experiments are: the attachment k_{att}, Freundlich distribution k_F, and dispersion coefficients D_p. Straining did not seem to influence the peak and time of peak, but it has an important role in explaining the tailing of the BTC. When parameters for ShortPAmCOM

were fitted, best-fit values (run 3a, $r^2 = 0.62$) were as follows: 6.45 mm^2 d^{-1}(D_p), 0.026 d^{-1} (k_{att}), and 125,8 mm^3 g^{-1} (k_F). Best-fit parameter values for LongPAmCOM were (run 3b, r^2 =0.77): 8.36 mm^2/d (D_p), 0.0088 d^{-1} (k_{att}), and 60 mm^3 g^{-1} (k_F).

CONCLUSIONS

Migration of colloidal OM in undisturbed clay cores was described by means of combining the advective-dispersive-retardation equation and attachment-detachment theory. By inverse modeling, best-fit parameter values were derived for the experimental setup with the OM source spiked in the middle. Forward modeling for the same setup, but with different flow rates, gave calculated breakthrough curves (BTC) in good agreement with the experimental data. The forward modeling failed, however, when applied to a different setup (tracer source at different location). For the latter case, additional inverse modeling produced parameter values quite different compared to the initial runs. Sensitivity analysis revealed the most influential parameters were the attachment, Freundlich sorption and dispersion coefficients. Straining had most influence on the tailing of the BTC. Results further suggest that colloid migration parameters are sensitive to the experimental setup, more specific to the spatial scale used in deriving parameter values. Therefore, extrapolation of parameter values obtained from small-scale core samples to large scale in-situ conditions must be done with care.

ACKNOWLEDGEMENTS

The work of A. Ionescu was financially supported by the IAEA within the framework of URL project TC INT/9/173 “Training in and Demonstration of Waste Disposal Technologies in Underground Research Facilities”.

REFERENCES

[1] N. Maes, L. Wang, G. Delécaut, T. Beauwens, M. Van Geet, M. Put, E. Weetjens, J. Marivoet, J. Van der Lee, P. Warwick, A. Hall, G. Walker, A. Maes, C. Bruggeman, D. Bennett, T. Hicks, J. Higgo, D. Galson, Migration case study: Transport of radionuclides in a reducing clay sediment (TRANCOM-II). Final scientific and technical report of the TRANCOM-II EC project, SCK·CEN-BLG-988, Mol, Belgium (2004).

[2] J. Simunek, M. Th. Van Genuchten, M. Sejna, The HYDRUS-1D Software package for simulating the One-dimensional movement of water, heat and multiple solutes in variably-saturated media, version 3.0 (2005).

[3] N. Maes, L. Wang, T. Hicks, D. Bennett, P. Warwick, T. Hall, G. Walker, A. Dierckx, The role of natural organic matter in the migration behaviour of americium in the Boom Clay – Part I: Migration experiments. Physics and Chemistry of the Earth 31, 541-547 (2006).

[4] S. A. Bradford, M. Bettahar, J. Simunek, M. Th. Van Genuchten, Straining and attachment of colloids in physically heterogeneous porous media, Vadose Zone J. 3:384-389 (2004)

[5] S. A. Bradford, J. Simunek, M. Bettahar, Y. F. Tadassa, M. Th. Van Genuchten, S.R. Yates, Straining of colloids at textural interfaces, Water Res. Research, vol. 41, W10404, (2005).

[6] A. Ionescu, Progress report no. 2, Internal report SCK-CEN, (2006).